Collective Dynamics in Human and Monkey Sensorimotor Cortex: Predicting Single Neuron Spikes

Supplementary Information

Wilson Truccolo[1,2,5], Leigh R. Hochberg[2-6] and John P. Donoghue[4,1,2]

[1]Department of Neuroscience, [2]Brown Institute for Brain Science and [3]Division of Engineering, Brown University, Providence, RI
[4]Rehabilitation Research and Development Service, Department of Veterans Affairs, Providence, RI
Departments of Neurology, [5]Massachusetts General, [6]Brigham and Women's, and Spaulding Rehabilitation Hospitals; Harvard Medical School, Boston, MA
Corresponding author: wilson_truccolo@brown.edu

A. Single and dual microelectrode array recordings

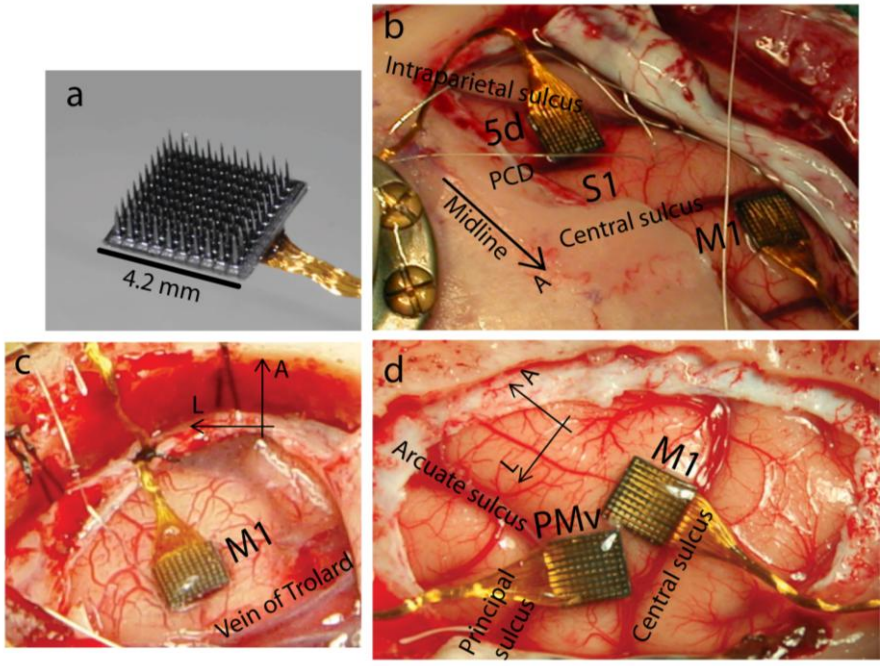

Supplementary Figure 1. Single and dual microelectrode array recordings from human and non-human primate sensorimotor cortex. Chronically implanted arrays are shown during the surgery. Recordings reported here were performed weeks to months after surgical implantation. **(a)** The 10 x 10 microelectrode array. The array's platform is 4.2 x 4.2 mm, with minimum inter-electrode distance of 400 μm. Maximum inter-electrode distance was ~ 2 cm (for electrodes in two arrays). **(b)** Dual array recordings: two implanted arrays in arm related areas of monkey primary motor (M1) and parietal (5d) cortex. PCD stands for posterior central dimple and "midline" corresponds to the sagittal suture. The arrow point to the anterior (A) direction. **(c)** Array implanted in the arm (knob) area of primary motor cortex, human subject hS3. The labeled vein of Trolard is a large superficial vein that runs atop the central sulcus. The arrows point to anterior and lateral (L) directions. **(d)** Dual array recordings from monkey M1 and ventral premotor (PMv) areas. The twelve datasets used in the analyses included 1,187 neuronal recordings: hS1 (n = 22, n = 21), hS3 (n = 108, n = 110), mLA (n = 45, n = 45), mCL (n = 47, session 1; n = 44, session 2), mCO (M1: n = 148, n = 109;

PMv: n = 77, n = 109) and mAB (M1: n = 104, n = 110; 5d: n = 41, n = 47). We did not distinguish whether a single unit sorted from the same electrode on different days corresponded to the same neuron or not.

B. Predictive power and ensemble size in M1

We conjectured (main text) that the smaller size of the M1 neuronal ensemble for participant hS1 (n=21, n=22) explained the lower predictive power obtained for this participant in comparison to hS3, mLA and mCL (Fig. 3, main text). To further investigate this possibility, we randomly sampled subsets of 22 neurons out of the 110 neuron ensemble from participant hS3 (session 2). Data from hS3 provided a good reference since these neurons were recorded from M1 under the same task condition. Twenty of these random subsets, each of size n = 22, were sampled. Although these subsets were different, some of the neurons could be present in multiple subsets. In each random subset, conditional intensity functions for each neuron were modeled as a function of the intrinsic spiking history and the spiking histories of the other neurons in the random subset. Predictive power of these history models for each target neuron was computed as in the main text. Supplementary Figure 2 shows the distribution of predictive power for all of the neurons in these 20 random subsets. This distribution was similar to the one obtained for hS1, supporting our conjecture.

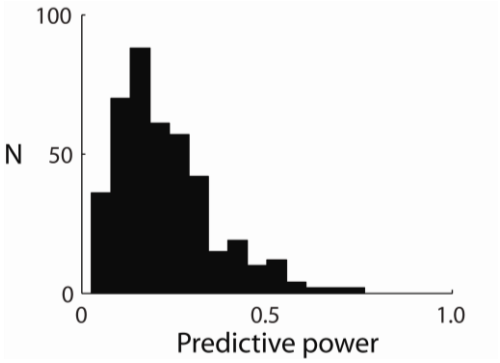

Supplementary Figure 2. Distribution of M1 (Intra-areal) ensemble predictive power: random ensemble subsets of size n = 22 (hS3, session 2).

C. Comparing the predictive power of spiking history and pathlet models (hand position and velocity trajectories) in M1, PMv and 5d neurons

M1 neurons are known to be strongly modulated with hand position and velocity during reaching movements, as performed in the task executed by the monkeys in this study (Ashe and Georgopoulos, 1994; Moran and Schwartz, 2001). In particular, Hatsopoulos et al. (2007) and Paninski et al. (2004) have shown that M1 neurons can be highly tuned to preferred trajectories in velocity space, that is, neurons are not only tuned to the instantaneous velocity at a particular single time lag, but are related to velocity trajectories spanning a short time period. This means that trajectories (histories) in velocity space can also predict single neuron spikes and could potentially account for the same predictive power observed for the ensemble history. We were interested in how the predictive power of recent spiking history compared to the predictive power of hand position and velocity trajectories. We used 'pathlet' models (Hatsopoulos et

al., 2007) to express the instantaneous spiking rate at time *t* as a function of the instantaneous hand position and velocities over the time interval [-200, 300] ms around neuron time *t*. Specifically, this 'pathlet' conditional intensity model was obtained from

$$\log\left[\lambda_i(t \mid p_{1,t+\tau}, p_{2,t+\tau}, v_{1,t+\tau_1:t+\tau_2}, v_{2,t+\tau_1:t+\tau_2})\Delta\right] = \mu_i + a_i p_{1,t+\tau} + b_i p_{2,t+\tau} + \sum_{k\in\{-4,-1,\ldots,6\}} c_{i,k} v_{1,t+k\delta} + d_{i,k} v_{2,t+k\delta} \ ,$$

where $p_{1,t+\tau}$ and $p_{2,t+\tau}$ are the positions in the horizontal and vertical coordinates at a preferred time lag $t+\tau$ (depending on the neuron), $v_{1,t+\tau_1:t+\tau_2}$ and $v_{2,t+\tau_1:t+\tau_2}$ correspond to the velocities over the time interval $[\tau_1 = -200, \tau_2 = 300]$ ms, sampled at $\delta = 50$ ms time steps; (pathlet models for *m*CO included position and velocity in 3 dimensions); a,*b,c* and *d* are tuning parameters estimated via maximum likelihood methods (Truccolo et al., 2005). The choice of the above time interval was based on the study in Hatsopoulos et al. (2007) and on exploration of different intervals in our own data; use of larger time intervals did not significantly improve prediction performance. Supplementary Figure 3 (top row) shows the distributions of predictive power values based on these pathlet models for neurons recorded from the four monkeys. The predictive power of full history models was typically higher than the predictive power of pathlet models.

We also examined the issue of redundancy between the information conveyed by spiking histories and information conveyed pathlet models (Supplementary Fig. 4). The following points summarize our analysis of this redundancy:

(a) If there was no redundancy in the information conveyed by these two models, the predictive powers of a history model and of a pathlet model for a given neuron should add to at most 1, the maximum possible value corresponding to perfect prediction. By contrast, the predictive powers of these two individual models were not strictly additive, i.e. they could add up to values greater than 1, indicating that some of the same spiking activity predicted by the spiking history models could also be predicted by the examined kinematics (Supplementary Fig. 4).

(b) This redundancy was also present for neurons whose summed predictive powers of spiking history and pathlet models added up to a value smaller than 1. The predictive power of a combined model (i.e. a model that included both spiking histories and kinematics) was significantly smaller than the sum of the predictive power of the two individual models for the majority of neurons (>80% of neurons in the 3 studied cortical areas).

(c) Despite the redundancy between the information conveyed by these two models as implied in (a,b), there was also extra information about single neuron spiking in the spiking history that could not be accounted for by the examined kinematics. This follows from the fact that predictive power was typically higher for spiking history models as seen in Supplementary Figure 3.

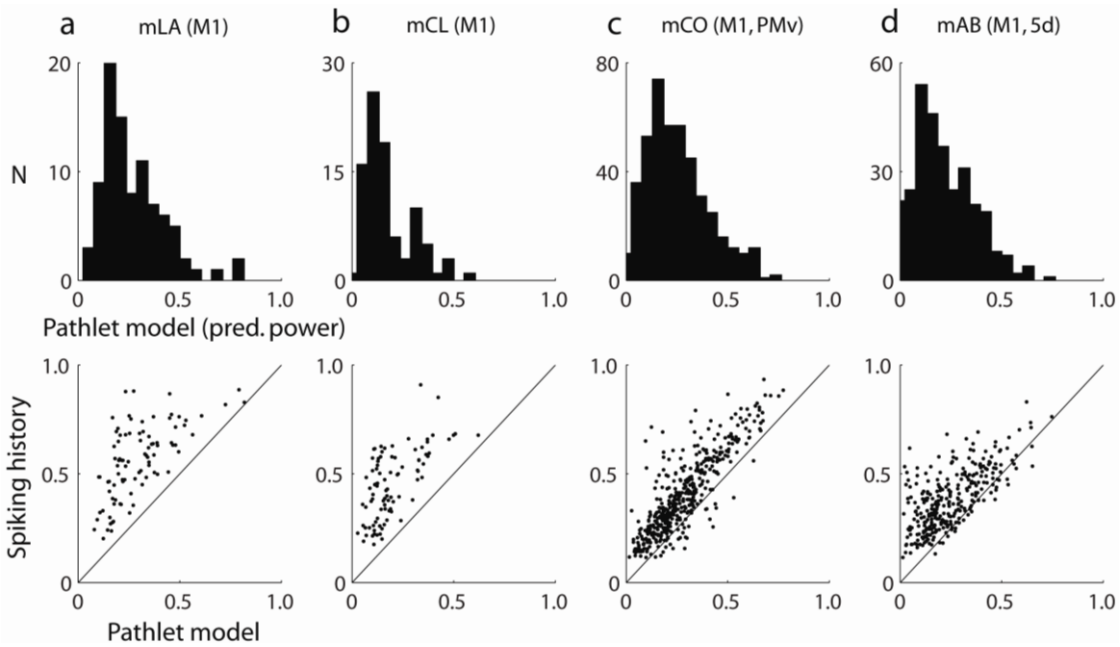

Supplementary Figure 3. Predictive power of spiking history models versus pathlet models. Top row shows the distributions of predictive power computed from the pathlet models for each of the four monkeys. The second row shows the predictive power of spiking history models versus the predictive power of pathlet models.

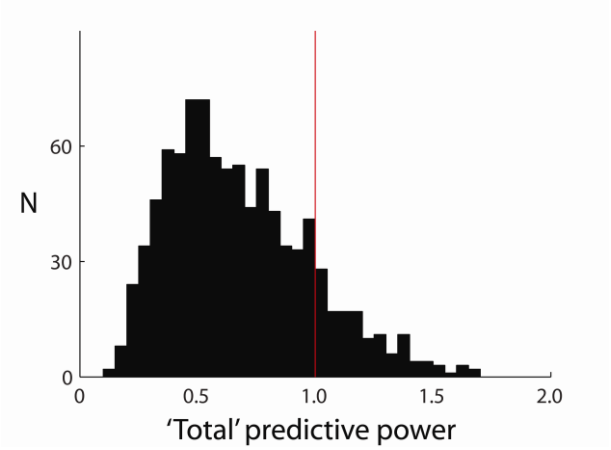

Supplementary Figure 4. Histograms of the 'total' predictive power of ensemble spiking history and pathlet models. Here, 'total' predictive power refers to the sum of the predictive power of the spiking history model and the power of the pathlet model, computed for each neuron (n = 924 neurons; datasets mLA, mCL, mCO and mAB). This 'total' predictive power should add up to at most 1 (perfect prediction) if there was no redundancy between the information conveyed by ensemble history models and the information conveyed by pathlet models.

D. Ensemble size and inter-areal predictive power

Further, we also investigated whether the larger number of neurons in M1 ensembles could explain the higher predictive power of inter-areal predictive power, in comparison to the intra-areal predictive power, especially for the M1 → PMv effect in some of the examined target neurons. To address this issue, we fitted new history models based on balanced-size ensembles, that is, the number of neurons in M1 and PMv

ensembles (and in the M1 and 5d ensembles) were set to be equal. First, we set the number of neurons *n* in the ensembles for both areas to equal the number of neurons in the smallest ensemble of the cortical pair: in our case, the number of neurons in 5d for the M1−5d pair, and PMv for the M1−PMv pair. Second, for each neuron whose spiking was to be predicted, we ranked the input neurons according to their strength based on the magnitudes of the corresponding original model coefficients: i.e., the coefficients estimated based on the full history models shown in Figure 5 (main text). We then included in the new *balanced-size* models only the *n* top-ranked neurons. Supplementary Figure 5 shows the differences between intra and inter-areal predictive power for target neurons in M1, PMv and 5d. Differences between intra and inter-areal predictive power in these balance ensembles were small on average. Nevertheless, especially for M1, the distribution of these differences was skewed toward positive values, i.e. higher values for intra-areal predictive power.

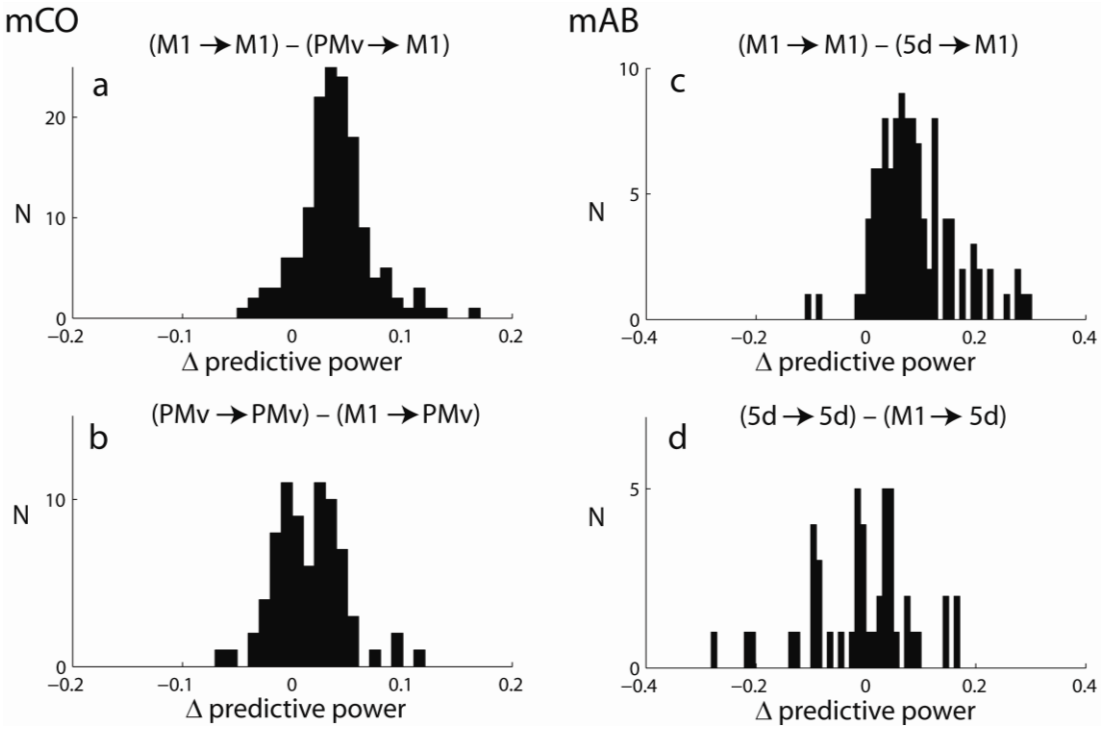

Supplementary Figure 5. Intra versus inter-areal predictive power for balanced-size ensembles. (a,b) and (**c,d**) show the comparisons for the M1−PMv and M1−5d pairs, respectively. The term "Δ rel. predictive power" denotes the difference between intra and inter-areal ensemble predictive power. For example, (PMv → PMv) − (M1 → PMv) represents the difference between the predictive power of intra-areal ensembles in PMv and inter-areal ensembles in M1 to predict single neuron spiking activity in PMv. Balanced-size ensembles: M1−PMv, n = 77 and n = 109, for sessions 1 and 2, respectively; M1−5d, n = 41 for both sessions.

Supplementary references

Ashe, J. & Georgopoulos, A.P. Movement parameters and neural activity in motor cortex and area-5. *Cereb. Cortex* **4**, 590–600 (1994).

Moran, D.W. & Schwartz, A.B. Motor cortical representation of speed and direction during reaching. *J. Neurophysiol.* **82**, 2676 –2692 (1999).

Hatsopoulos, N.G., Xu, Q. & Amit, Y. Encoding of movement fragments in the motor cortex. *J. Neurosci*. **27**(19), 5105-5114 (2007).

Paninski, L., Fellows, M. R., Hatsopoulos, N. G., & Donoghue J. P. Spatiotemporal tuning of motor neurons for hand position and velocity. *J. Neurophysiol.* **91**, 515–532 (2004).

Truccolo, W., Eden, U.T., Fellows, M.R., Donoghue, J.P. & Brown, E.N. A point process framework for relating neural spiking activity to spiking history, neural ensemble, and extrinsic covariate effects. *J. Neurophysiol*. **93**, 1074 –1089 (2005).